



Swansea University
Prifysgol Abertawe



Cronfa - Swansea University Open Access Repository

This is an author produced version of a paper published in:
Structural and Multidisciplinary Optimization

Cronfa URL for this paper:
<http://cronfa.swan.ac.uk/Record/cronfa40978>

Paper:

Aldoumani, N., Haddad Khodaparast, H., Giannetti, C., Abdallah, Z., Cameron, I., Friswell, M. & Sienz, J. (2018). A robust design of an innovative shaped rebar system using a novel uncertainty model. *Structural and Multidisciplinary Optimization*, 58(4), 1351-1365.

<http://dx.doi.org/10.1007/s00158-018-2050-z>

This item is brought to you by Swansea University. Any person downloading material is agreeing to abide by the terms of the repository licence. Copies of full text items may be used or reproduced in any format or medium, without prior permission for personal research or study, educational or non-commercial purposes only. The copyright for any work remains with the original author unless otherwise specified. The full-text must not be sold in any format or medium without the formal permission of the copyright holder.

Permission for multiple reproductions should be obtained from the original author.

Authors are personally responsible for adhering to copyright and publisher restrictions when uploading content to the repository.

<http://www.swansea.ac.uk/library/researchsupport/ris-support/>



A robust design of an innovative shaped rebar system using a novel uncertainty model

Nada Aldoumani¹ · Hamed Haddad Khodaparast¹ · Cinzia Giannetti¹ · Zakaria Abdallah¹ · Ian M. Cameron¹ · Michael I. Friswell¹ · Johann Sienz¹

Received: 6 April 2018 / Revised: 9 July 2018 / Accepted: 10 July 2018 / Published online: 17 August 2018
© The Author(s) 2018

Abstract

The current paper has investigated a newly developed re-bar system by implementing uncertainty models to optimise its geometry. The study of the design parameters of this re-bar system has been carried out utilising a novel uncertainty model that has been developed at Swansea University. The importance of this invention comes from the fact that the whole process of optimisation has been automated by linking ANSYS Workbench to MATLAB via the in-house written code. Despite the fact that in the past, ANSYS APDL was linked to MATLAB, however, the APDL was very limited to only simple geometries and boundary conditions unlike the Workbench which can simulate complex features. These shortfalls have been overcome by automating the process of optimisation, identifying the key influential parameters and the possibility to carry out a huge number of trials. Moreover, the tools that have been developed can pave the way for robust optimisation of this proposed structure. The uncertainty in the design parameters of this re-bar system is of a paramount importance in order to optimise the bond strength between the newly developed rebar and the concrete matrix as well as to fully understand the behaviour of the proposed system under pull-out conditions. The interface between the rebar and the concrete matrix was considered as a ‘cohesive zone’ whereby the interfacial area is studied as a function of the bonding strength.

Keywords Robust design · Rebar systems · Bond strength · Concrete · Uncertainty · ANSYS · MATLAB

1 Introduction

For an optimal design of reinforced concrete structures, efficient and reliable transfer of stresses between the reinforcement and the concrete is required. The transfer of such stresses from the reinforcement to the surrounding concrete takes place once the reinforcement deforms. In other words, after the initial slip of the bar, the stresses are transferred by bearing friction, as shown in Fig. 1. The transfer of the axial force from the reinforcing steel bars to the surrounding matrix is facilitated by the development of tangential stresses along the interfacial area and these are the necessary bond stress to hold the components

together. This means that the bond strength is dependent on the interaction between the steel bar and the surrounding matrix. Moreover, it depends on the mechanical properties of the concrete, volume of concrete around the bars, the surface condition of the bar alongside the geometry of the bar. Moreover, it relies on the diameter of the bars alongside the loading age (ACI Committee 2016). The design of conventional bar systems includes ‘ribs’ of certain size and shape. These ribs play a key role in the transfer of stresses between the reinforcement and the surrounding matrix. For instance, for plain bars, the failure occurs due to the loss of adhesion between the bars and the cement paste. This means that the failure stress is proportional to the interface area between the two constituents. On the other hand, when ribs are used, strength in the slipping is due, mainly, to the strength that the concrete offers to the pressures exercised on it by the ribs. This means that the chemical adhesion has a less importance in this case when compared to the mechanical interaction between the ribs and the surrounding matrix (Barbosa et al. 2008).

Overall, the plain systems rely on the adhesion as well as friction whereas those are of less importance in deformed bars

Responsible Editor: W. H. Zhang

✉ Zakaria Abdallah
z.a.m.abdallah@swansea.ac.uk

¹ The Advanced Sustainable Manufacturing Technologies (ASTUTE) Project, College of Engineering, Swansea University, Fabian Way, Swansea SA1 8EN, UK

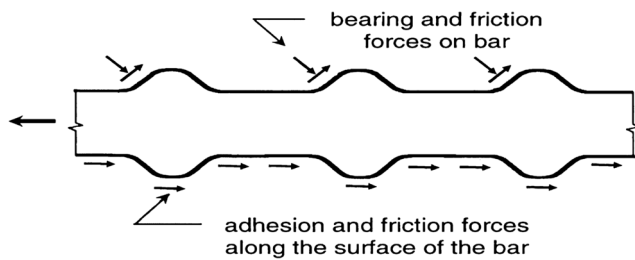


Fig. 1 A deformed bar during the transfer of forces from the reinforcement to the surrounding concrete (ACI Committee 2016)

with ribs wherein the effect of mechanical interlocking and shear along the interfacial area are of utmost importance. The surface roughness and the closely spaced ribs produce great interlocking with good bearing effects. In the same context, the stress parallel to the bar is termed as the ‘bond stress’ whereas that perpendicular to the contact surface is called the ‘radial stress’. There has been an extensive research on the effect of the resultant stress of the combined bond stress and the radial stress in such structures. It has been revealed that changing the stresses in the parallel and transverse directions has resulted in the formation of primary and secondary cracks in the concrete adjacent to the bar, Fig. 2, (Kabir and Islam 2014).

It is possible to increase the bond between the bar and the concrete by increasing the surface area of the bar whereby a larger bonding strength is obtained. This requires re-shaping the currently employed standard bars in such a way that provides increased bond strength. Many research studies have concentrated on the shape of the rebar system as well as the aspect ratio of the steel with respect to the cross sectional dimension. The addition of some features such as the dovetail

design that provides an increased lateral surface area is the main scope of the Co-tropic rebar systems. This dovetail design is not a material dependent. In other words, it can be applied to other materials that can be extruded and drawn to size. The shape of this rebar system contains multiple re-entrant dovetail-shaped grooves in which the open end of the groove is narrower than the closed end of the groove. This modification of the shape has increased the surface area by 1.9 times the conventional solid round rebars of an equivalent diameter (Thomas 2011). This modern design of the Co-tropic rebar system provides an ‘interlocking’ feature that makes use of the positive Poisson’s ratio contraction when the rebar is subjected to tensile loading. When the rebar is under tensile loads, only the tops of ridges or surface of the fibres will debond while the sides of the dovetail grooves contract inwards and squeeze the concrete within the groove, as shown in Fig. 3a) and Fig. 3b). This action provides an improved bonding strength in contrast to the conventional systems whereby the stretching of the solid round bar can result in an interfacial separation from the matrix Fig. 3c) and Fig. 3d), (Thomas 2011).

The main scope of the current paper is to explore the sensitivity of the various parameters in the newly developed rebar system. That is, the performance of the bonding strength between the rebar system and the surrounding matrix is influenced by many parameters such as the outer radius of the rebar system, the groove radius, the distance between the centre of the rebar shape to the centre of the cutout shape, the radius of the edges alongside the angle from one edge to the successive edge within the same groove. This exercise will employ uncertainty studies using an innovative model that has been developed at Swansea University. In this regard, it has become

Fig. 2 (a) Force components parallel and perpendicular to the steel concrete interface (b) Shear stress distribution in XY plane of concrete (Kabir & Islam 2014)

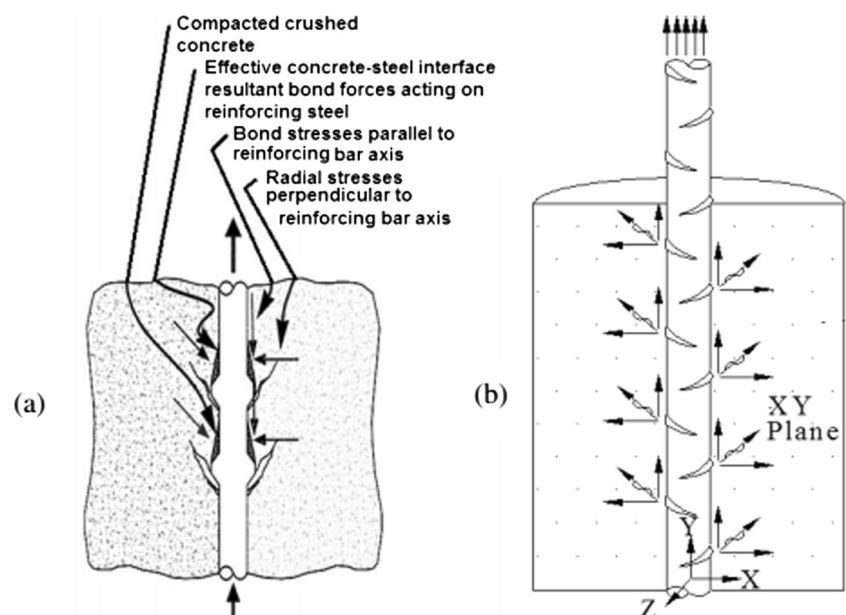
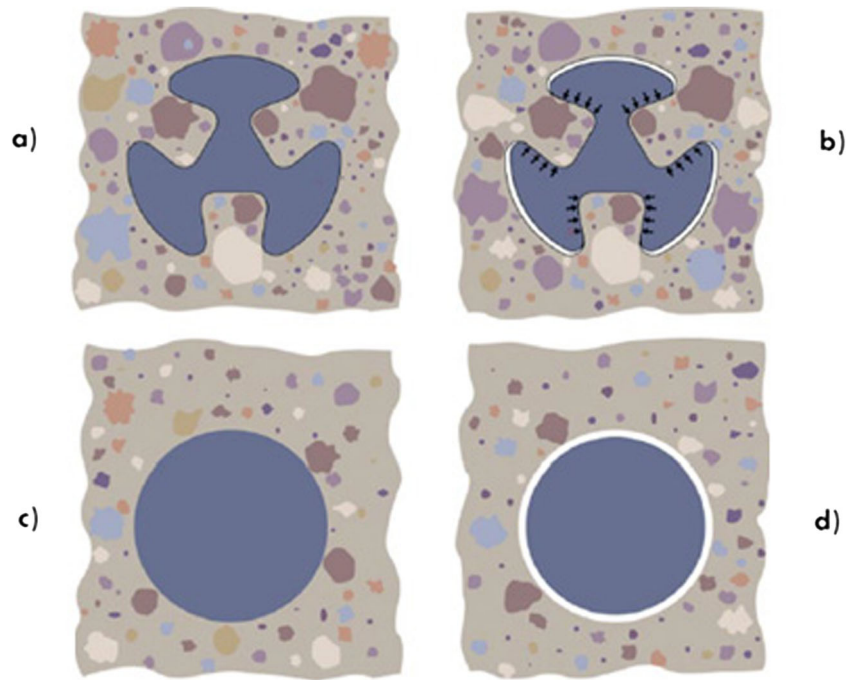


Fig. 3 A comparison between the Co-tropic dovetail-shaped system and the conventional rebar system: (a) the Co-tropic rebar with no load, (b) the Co-tropic rebar stretched, (c) the conventional rebar with no load, and (d) the conventional rebar stretched (Thomas 2011)



possible to link ANSYS Workbench via MATLAB using an in-house written code that has been examined and provided precise results. Yet, this paper presents the first publication in a series of future publications utilising this novel method which can open new eras of collaborative research in future. The advantage of this developed routine is that it allows the user to enter as many input parameters as required whereby the code will automatically operate the ANSYS, run the model, get the results and feedback to obtain other results. This means that any parameter, such as the outer radius in the newly developed rebar system, can be chosen as a set of random values within a defined range from which the bond strength, for instance, of the structure can be evaluated. This allows the possibility of choosing the most sensitive parameters alongside the values that provide the optimum bond strength. This will reduce the time, cost and number of trials to choose the optimum design parameters alongside the use of mathematical tools such as the Meta-models in conjunction with this code for efficient uncertainty analysis.

2 The employed parameters in the design

The material properties of the modelled concrete and steel have been obtained from literature studies (Shafaie et al. 2009) as summarised in Table 1. These mechanical properties will be employed in the analysis of the pull-out test from which comparisons between the experimental and the simulated results can be obtained. Once the simulated results are shown to approximate

the experimental results by changing certain parameters in the model, it can thereafter be described as being ‘validated’ for similar applications.

The experimental results carried out elsewhere (Shafaie et al. 2009) on standard steel bars bonded to concrete structure under pull-out conditions were utilised in this paper in order to verify and validate the generated model that will be applied to the Co-tropic rebar system. In the same study of Shafaie et al., a steel bar of 12 mm diameter with a cross sectional area of 113 mm² has been tested. The steel bar was contained within a 90 mm high cylindrical concrete structure of 60 mm diameter with an anchorage depth of 60 mm. The obtained results will be compared with those obtained for the Co-tropic rebar system such that optimisation and uncertainty studies can thereafter be carried out.

Table 1 A summary of the materials properties utilised in the current study (Shafaie et al. 2009)

Material Properties	Values (kg/cm ²)
Concrete compressive strength	300
Concrete tensile strength	30
Concrete E modulus	273,664
Concrete Poisson’s coefficient	0.2
Steel E modulus	2,100,000
Steel yield stress	3000
Steel Poisson’s coefficient	0.3

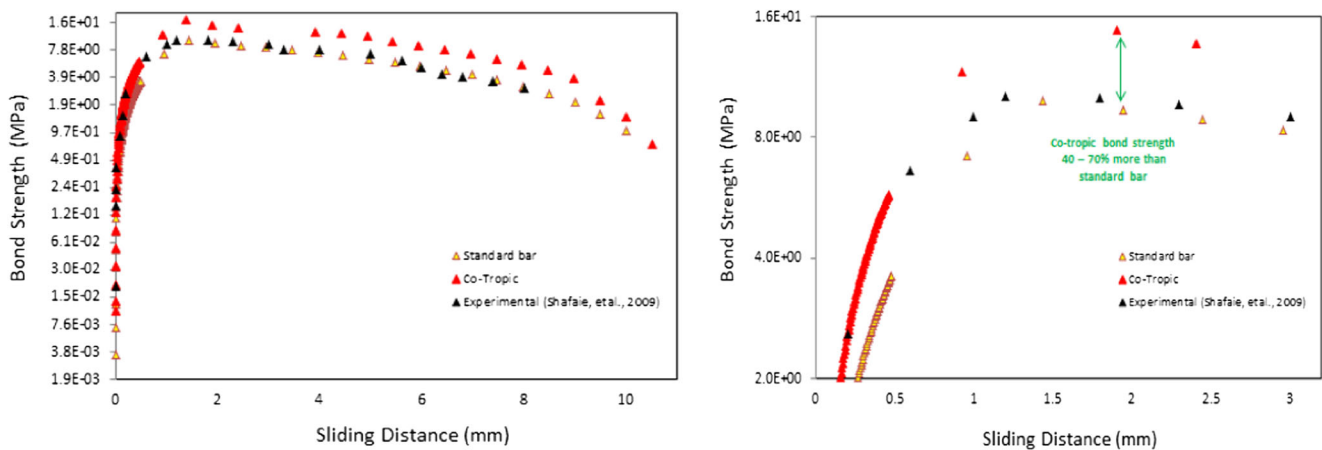


Fig. 4 The simulation results of the standard rebar and the Co-tropic rebar systems carried out at Swansea University compared to the experimental pull-out test results conducted elsewhere (Shafaie et al. 2009) on standard bar systems

3 The ANSYS model

The ANSYS 16.2 Workbench finite element (FE) package was used to carry out the modeling. The applied load was iterated step by step using the Newton-Raphson method. In this paper, SOLID185 has been used for the modeling of the steel bar and concrete. It has been defined by eight nodes having three degrees of freedom at each node and translations in the nodal x , y , and z directions. The element has plasticity, hyperelasticity, stress stiffening, creep, large deflection and large strain capabilities. It also has mixed formulation capability for simulating deformations of nearly incompressible elastoplastic materials and fully incompressible hyperelastic materials (Mahmoud 2016). At the interface of the steel rebar and the concrete, interface elements have been employed whereby the steel rebar surface is treated as the “target” surface and simulated using element TARGE170 while the concrete surface is treated as the “contact” surface and simulated by element CONTA174. The target elements and contact elements must be set to

the same real constant number. These elements are able to simulate the existence of pressure between them when there is either a contact or separation between them. The two material contacts also take into account the cohesion between the involved parameters (ANSYS Inc. 2012). Such elements allow the separation of the bonded contact to simulate the delamination of the interface. Moreover, they are considered higher order elements that are able to provide more accurate results for quadrilateral mesh and can tolerate irregular shapes without much loss of accuracy. The Pure Penalty Method (penetration and no sliding) (Doyle 2012; ANSYS 2010; You 2013) has been used in the tangential direction while using the conditions of the Lagrange Multiplier method which involves sliding with no penetration according to (ANSYS 2010):

$$F_{\text{tangential}} = K_{\text{tangential}} \cdot X_{\text{sliding}}$$

Where $F_{\text{tangential}}$ is the tangential force between the surfaces, $K_{\text{tangential}}$ is the tangential stiffness between the

Fig. 5 The meshing of the Co-tropic rebar system with fine mesh nearby the region of interest while a coarser mesh is employed for the farther regions from the cohesive zone area

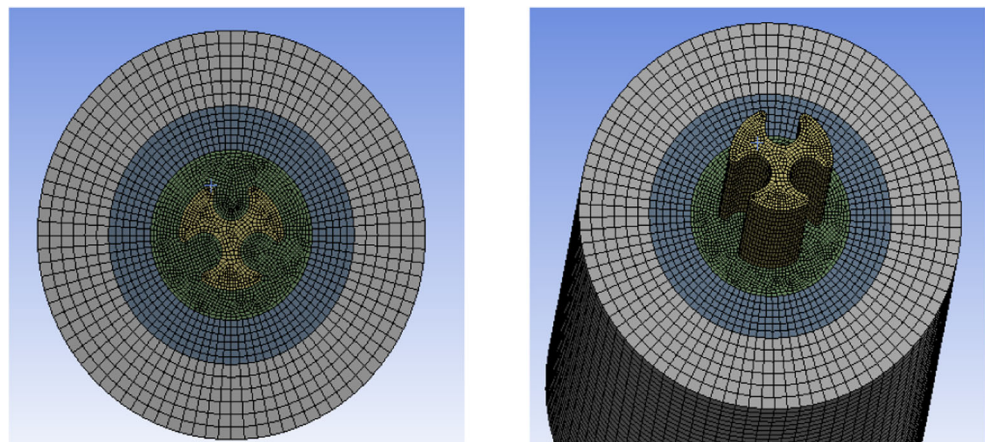
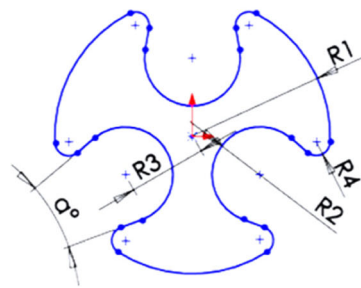


Fig. 6 The parameters of interest in the Co-tropic rebar system that have been investigated



R1: The outer radius of the rebar system.

R2: The groove radius.

R3: The distance between the centre of the rebar shape to the centre of the cutout shape.

R4: The radius of the edges

α : The angle from one edge to the successive edge within the same groove.

surfaces and $X_{sliding}$ is the sliding distance as a result of the applied force. The value of $X_{sliding}$ is ideally zero for sticking conditions, however, some slip is allowed in our case. This will require chattering control parameters as well as a maximum allowable elastic slip (ELSI) parameter (i.e. $K_{tangential}$), (Doan 2013). In addition to the above boundary conditions, the ‘cohesive zone material’ model has been used to model the delamination process of the interface (i.e. debonding). The adhesion properties of the utilised adhesive were entered via the ‘cohesive zone material model’ with ‘bi-linear’ behaviour mode and these were allocated for the contact elements of the model. To define a bi-linear material’s behaviour of adhesion, the separation distance and the constant properties of the adhesive material, the TBDATA command in ANSYS was used. In this case, the properties of the concrete have been defined by the user (ANSYS 2009; ANSYS 2012).

4 The robust design and uncertainty analysis

Research studies by Bryne and Taguchi and colleagues represent the first efforts in developing robust designs. They have introduced methods to minimise the effect of uncontrollable parameters during the design stage (Bryne 1987; Taguchi 1989). Further studies by Ross and colleagues employed the Taguchi loss function to make the design more tolerable to model variations (Ross 1995). Other researchers proposed

methods to reduce the variations in input parameters to obtain designs with lower sensitivities to design parameters (Ramakrishnan 1991). They have suggested a method for robust design with the Taguchi loss function as the object that is subjected to the model constraints. This allows the constant and variable sensitivities from controllable and uncontrollable parameters to be reduced using non-linear analysis. On the other hand, Padulo has investigated two main approaches for robust optimization in which the parameters are stochastic. The purpose of uncertainty in this case was to identify the uncertainties in input and output of a system or simulation tool (Padulo 2008). In structural analysis, it has become essential to determine the relationship between the various parameters with respect to the component geometry, the applied load, the material properties, and the contour conditions. In general, the main sources of uncertainty are associated with the properties of the adhesive, the geometry, material, load direction alongside many other factors (Neto and Rosa 2008). Other scholars have extended the use of uncertainty models on various materials and structures which has facilitated the design and optimisation exercise of structures (Wang and Al 2018a), (Wang and Al 2018b), (Wang and Al 2017a), (Wang and Al 2017b).

In this paper, the shape of the bar has been explored for the analysis. Various parameters have been investigated after which the most sensitive ones have been considered. In this context, 1000 random runs of the chosen parameters have been carried out from the space of input parameters. The

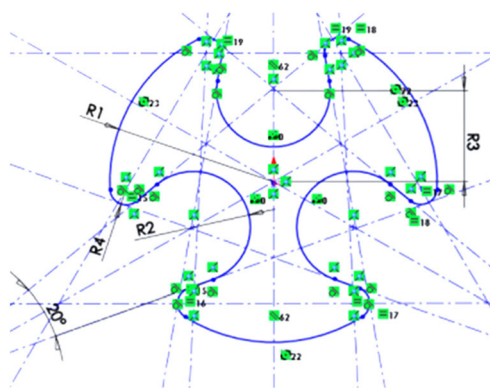


Fig. 7 The process of adding constraints to the geometry of the Co-tropic design while changing the design parameters

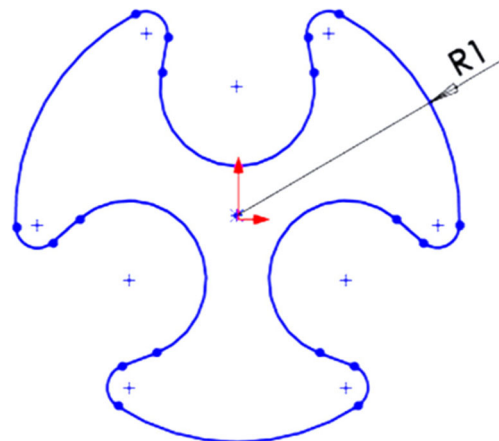
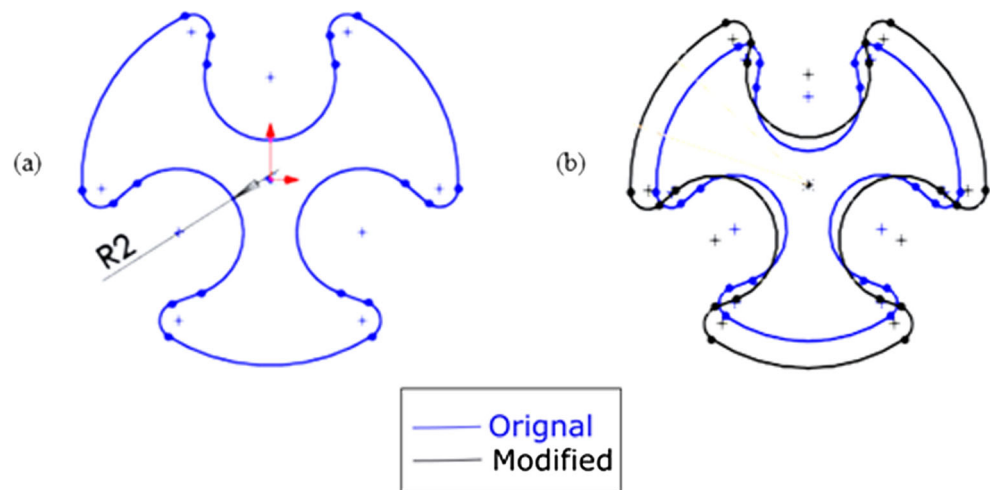


Fig. 8 The definition of $R1$ in the Co-tropic rebar system

Fig. 9 An illustration of: (a) The definition of R2 in the Co-tropic rebar system and, (b) The effect of altering R2 on the overall geometry when constraints are added



utilisation of 1000 trials was based on the fact that beyond this number the results would make no significant improvement as they have already converged at around the 1000th trial. The Monte Carlo simulation approach has been employed to obtain the corresponding 1000 outputs which represent the bonding strength of the structure. Afterwards, the Kernel probability distribution function has been estimated from the sample data using the Kernel Smoothing density function in MATLAB (R2013b). Regions of the acceptable output bonding strength were defined such that the bonding strength in those regions is desired for the design. The new advancement in the current paper is the creation of an automated script file that allows the designer to modify the parameters of complex geometries without the need to work with the ANSYS environment. That is to say, the MATLAB and ANSYS workbench interact with each other and the parameters are modified following this approach. This allows more flexibility to deal with complex geometries since this was, in the past, only restricted to simple designs. The framework for robust design proposed and employed by the same authors on carbon fibre composite materials bonded to aluminium connectors has recently been published elsewhere (Aldoumani et al. 2016). The code can be used for any future collaborative work on any engineering application that involves uncertainties in the design, manufacturing and operating conditions.

5 Results and discussion

5.1 The validity of the employed model

The model has first been validated under pull-out conditions using experimental data from literature studies (Shafaie et al. 2009). In the study of Shafaie et al., the numerical investigations were conducted using the finite element software ANSYS and have used a detailed model in 3D mode with and without the bond-slip effects. A cohesive layer was

employed to simulate the bond behaviour. Since the ribs were simulated, the mesh size close to the rib in the steel bar, concrete and cohesion layer was small enough to accurately describe the deformation and stress gradients. However, the remaining parts of the geometry contained a coarser mesh size in order to reduce the computational costs. The obtained results in their study have shown a significant consistency between the experimental data and the analytical simulations in terms of the trend of the bond behaviour. However, there was a slight reduction of about 10% in the bond strength in the calculated results when compared to the actual measurements. Even though, the simulation results were quite promising despite the small variation in the bond strength. On the other hand, when the standard rebar system, i.e. with ribs, was simulated at Swansea University using the same parameters employed elsewhere (Shafaie et al. 2009) under pull-out conditions, the results were extremely identical to those obtained experimentally by Shafaie et al., Fig. 4, with less than 2% error between the experimental data and the model developed during this study. This means that the employed model in the present study proved to be more precise than those employed in the other research studies. This has provided more

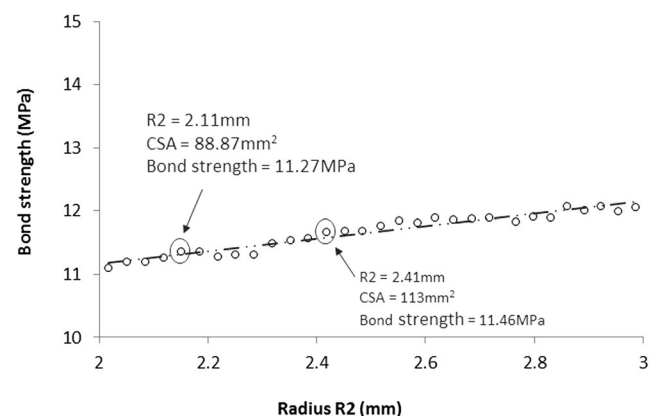


Fig. 10 The effect of modifying R2 on the bond strength of the Co-tropic rebar system

confidence in the model that will be applied to the Co-tropic rebar system. The results of the simulation using this model on the Co-tropic rebar have revealed that this novel system provides a higher strength in excess of 40–70% when compared to the conventional rebar system. In other words, the new geometry provided by the Co-tropic system has a direct influence on the bond strength to the concrete and hence the overall performance of the reinforced concrete.

5.2 The investigated parameters in the co-tropic rebar system

In order to obtain precise results from the simulation, the mesh size varied from the interface area to the outer regions of the structures. In other words, a very fine mesh was created for the Co-tropic rebar, interfacial area and the surrounding matrix nearby the rebar region. Away from this region, the mesh size was increased in order to reduce the time required to complete the analysis. The fine mesh will ensure that the cohesive zone region which is of utmost interest will provide very precise results when such a fine mesh is employed. At the outer regions, the deformation and analysis is of less importance hence the mesh has been coarser, Fig. 5.

A parameterisation process has been employed such that each parameter in the geometry is studied separately in order to determine the most significant parameters that affect the bonding strength of the rebar and the concrete. The parameters that were studied in the current project are R1, R2, R3, R4 and α as shown in Fig. 6. This method also allows the shape to be optimised in order to obtain the highest bond strength at the interface between the rebar and the surrounding concrete matrix. The definition of each parameter will shortly be covered in the current paper.

In order to obtain consistent results under all simulation conditions, the geometry has been constrained such that under any variation in any of the parameters, the shape of the rebar remains the same. This was possible using the CAD software in order to maintain a similar geometry for all simulations

Fig. 11 (a) the definition of R3 in the Co-tropic rebar system and, (b) the effect of altering R3 on the overall geometry when constraints are added

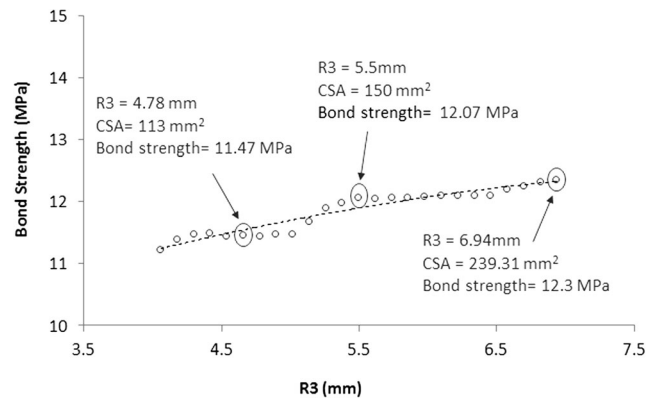
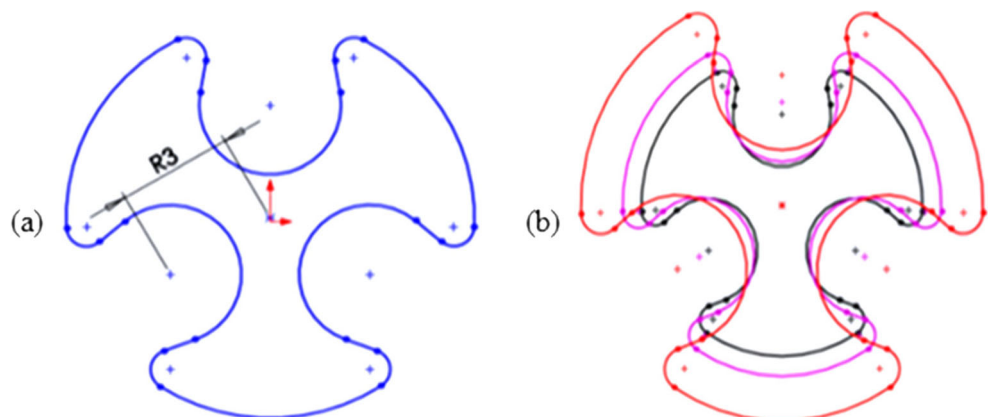


Fig. 12 The effect of modifying R3 on the bond strength of the Co-tropic rebar system

while the parameters are altered. The reason for the use of this constraint is that when the parameters were altered at the initial trials, the shape of the rebar has completely been modified, i.e. becomes completely different from the dovetail design. This would have been unacceptable since it does not help with the scope of the current paper as well as will not provide an optimisation of the parameters under investigation. The axes of constrains for the dovetail rebar system are shown in Fig. 7.

5.3 The sensitivity study of the parameters

The outer radius R1, shown in Fig. 8, is the distance from the centre of the rebar to the tangent of the outer surface. This parameter has a direct influence on the cross sectional area of the bar in addition to having an effect on the outer interfacial surface area which represents the boundary between the rebar and the concrete. The larger the outer surface area the better the bonding strength between the rebar and the surrounding matrix. For instance, when R1 was taken as 8.0 mm, the cross sectional area of the rebar was 113.0 mm² in comparison to 312.0 mm² when R1 was taken as 12.0 mm. In other words, it is clear that any increase in R1 will always increase the bonding strength due to the increased outer

surface area and hence the interfacial bond. For this reason, the variation of R1 was not considered in the analysis since it only provides basic information that can be easily drawn without the need for any further simulation.

On the other hand, the parameter R2 is the groove radius which represents the radius of the cut-out groove, Fig. 9a). In Fig. 9b), the effect of adding constraints to the geometry of the rebar system can be more clearly seen. In this figure, it can be seen even though the value of R2 has been altered, the geometry of the rebar system is maintained which is a great advantage in the current optimisation exercise.

The range of R2 within which the study was carried out was between 2.0–3.0 mm in order to not significantly increase the cross sectional area of the rebar system. The influence of changing R2 can be seen in Fig. 10, wherein the light-blue coloured text presents information about the point which represents the original shape of a cross sectional area of 113.0 mm² whereas the black coloured text is related to that calculated when R2 was taken as 2.11 mm with a cross sectional area of 88.87 mm². In terms of bond strength, the reduction of R2 has resulted in a reduction in the interfacial bond strength which is undesirable. This means that the gripping effect continuously decreases when R2 is decreased. Overall, when looking at the whole graph, it can be seen that the effect of reducing R2 has a minimal effect on the bond strength. In other words, the value of the bond strength is not significantly sensitive to the change in R2 which makes this parameter of less interest in the current analysis. The chosen range between 2.0–3.0 mm ensures that the ‘butterfly’ shape of the rebar remains the same as beyond this range the geometry will be modified which is undesirable.

On the other hand, the distance R3 is defined in Fig. 11 (a) as the distance between the centre of the rebar to the centre of the cut-out groove. The effect of constraints is shown in Fig. 11 (b) wherein the alteration of R3 affects the various parameters; however, the overall shape of the Co-tropic rebar is maintained.

Fig. 13 (a) the definition of R4 in the Co-tropic rebar system and, (b) the effect of altering R4 on the overall geometry when constraints are added

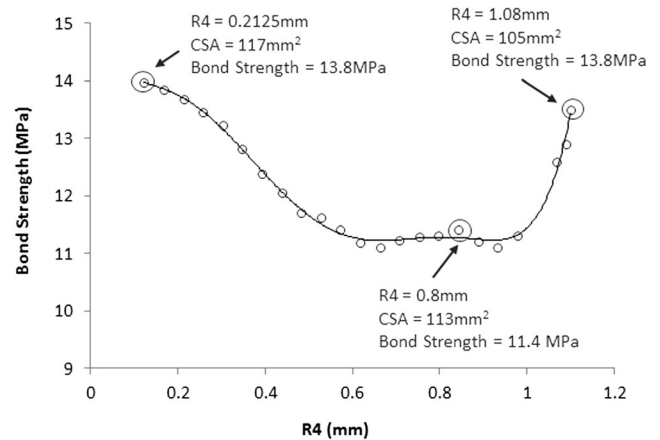
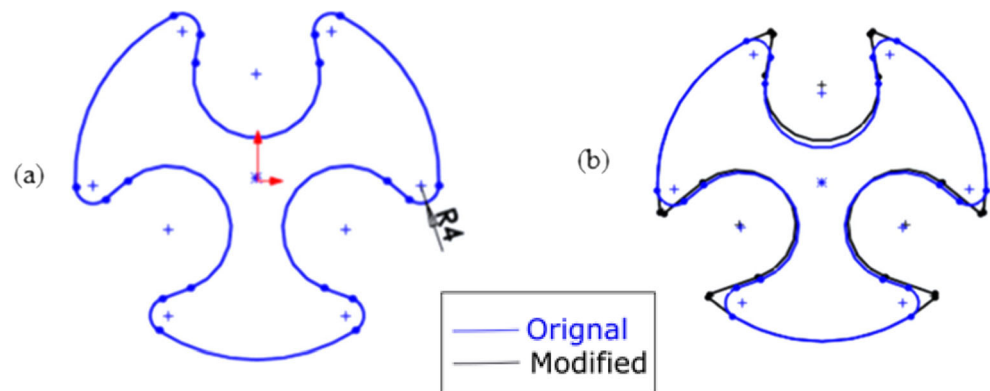


Fig. 14 The effect of modifying R4 on the bond strength of the Co-tropic rebar system

The influence of R3 on the overall bond strength is summarised in Fig. 12. It is evident that any decrease in R3 results in a significant decrease in the cross sectional area with a minimal decrease in the bond strength, i.e. the gripping effect. This means that the reduction of R3 leads to a reduction in the interfacial area between the rebar and the surrounding matrix and therefore provides a reduced bonding strength of the structure. This makes this parameter of less interest as it does not significantly affect the overall bond strength of the rebar system. It is worthwhile mentioning that the original shape in Fig. 12 is that with an area of 113.0 mm² (i.e. the black coloured measurement).

The radius R4, Fig. 13 (a), is defined as the radius of the edges and this has also been studied in order to investigate the effect of the shape of the edge shape on the overall bond strength. This parameter represents the ‘grips’ of the rebar that penetrate into the concrete matrix preventing it from excessive sliding. It is expected that the sharper the edges the better the capability of the rebar to grip into the concrete. This is due to the fact that the sharper the edges the smaller the area at the edge point and hence the higher the concentrated stress onto the concrete. The effect of modifying R4 is summarised in Fig. 13 (b) wherein it is evident that any decrease in R4 will

result in sharper edges. In this figure, the original shape is the light blue coloured dovetail of a cross sectional area of 113.0 mm² whereas that which has been modified with sharper edges, i.e. smaller R4, is plotted in black. The modification of R4 has caused a slight modification to the overall rebar design; however, the basic geometry of the dovetail is maintained due to the applied constraints.

The relation between R4 and the bond strength is summarised in Fig. 14. The bond strength is significantly influenced by the change in R4 when looking at the initial geometry of 113.0 mm². It can be seen that the decrease in R4 leads to a significant improvement in terms of the bond strength reaching a value of 13.8 MPa. Similarly, the increase in R4 starting from the initial geometry has also resulted in an increase of the bond strength reaching a value of 13.5 MPa. This means that this parameter can improve the bond strength without causing an excessive increase/decrease in the cross sectional area as can be seen in the three circled trials in Fig. 14. This makes this parameter worth investigating in terms of uncertainty and robust design as will be shown later in the current study.

The final parameter that has been investigated is the angle from one edge to the successive edge within the same groove and this is termed as ‘ α ’ as shown in Fig. 15 (a). This angle defines the amount by which the groove closes around the concrete. The ‘closing’ effect of the grooves can be understood in Fig. 15 (b) wherein the increase in the groove angle α brings the edges closer to one another, e.g. the black geometry in Fig. 15 (b) has an angle $\alpha = 41^\circ$ when compared to the original geometry in blue of an angle value $\alpha = 20^\circ$.

On the other hand, the sensitivity study of the feature angle α is shown in Fig. 16 by plotting the bond strength against this parameter. It is apparent that with increasing the angle α , the gripping effect also increases as indicated by the trend line, i.e. dashed line, leading to an increase in the bond strength. This effect takes place whilst the cross sectional area remains almost constant which is a great advantage to maintain the same

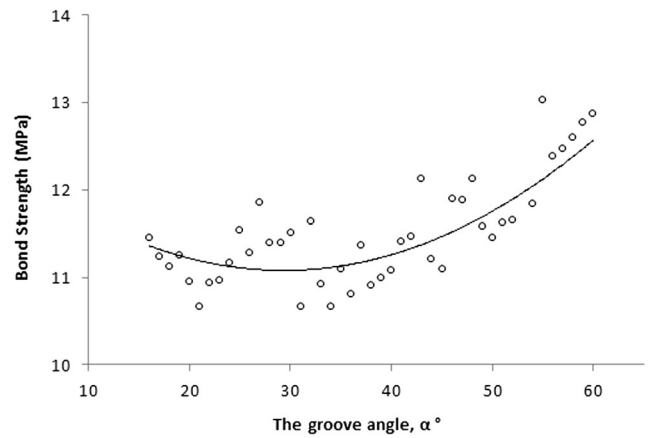


Fig. 16 The effect of modifying the feature angle α on the bond strength of the Co-tropic rebar system

geometry. Yet, the limitation of this parameter is that the central part of the bar becomes significantly thinner when increasing the value of α which will result in an increased stress at the central part of the rebar. This means that the bar itself might fail at a much lower stress than anticipated. Despite the fact that this might be the case, the scope of this paper is to investigate the overall bond strength and not the mechanical properties of the rebar which might be another topic for future studies. The change in α has resulted in a significant improvement of the bond strength and therefore, this parameter will be considered for further exploration in the current work.

5.4 The uncertainty and optimisation of the chosen parameters

The uncertainty exercise was carried out by maintaining the original values of R1, R2 and R3 as 8, 2.41 and 4.78 mm, respectively, obtained when the original area is 113mm². The range of variations for the uncertain parameters, i.e. R4 and α , utilised in the current analysis is shown in Fig. 14 and Fig. 16. From the probability distribution, Fig. 17 it is clear that more than one

Fig. 15 (a) the definition of α in the Co-tropic rebar system and, (b) the effect of altering α on the overall geometry when constraints are added

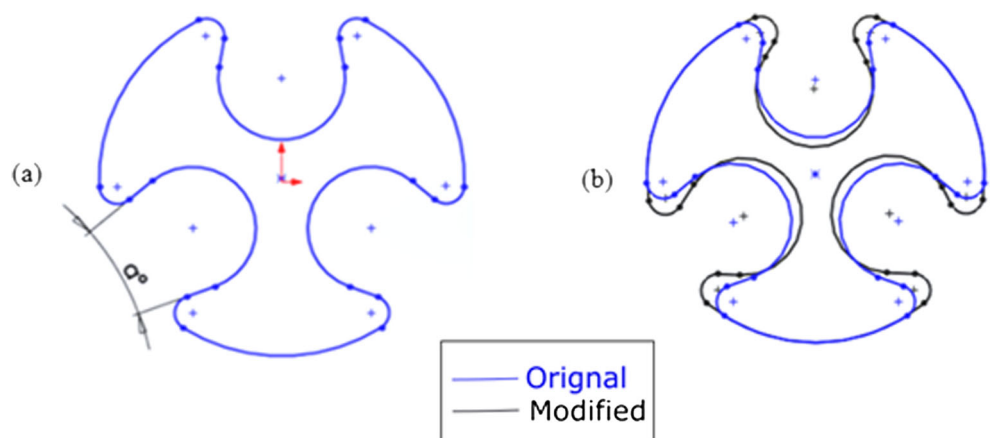
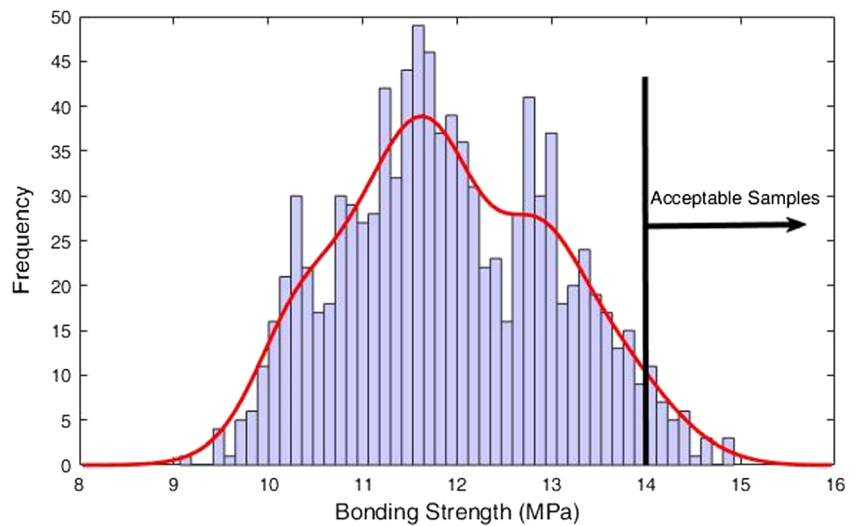


Fig. 17 The probability distribution of the samples



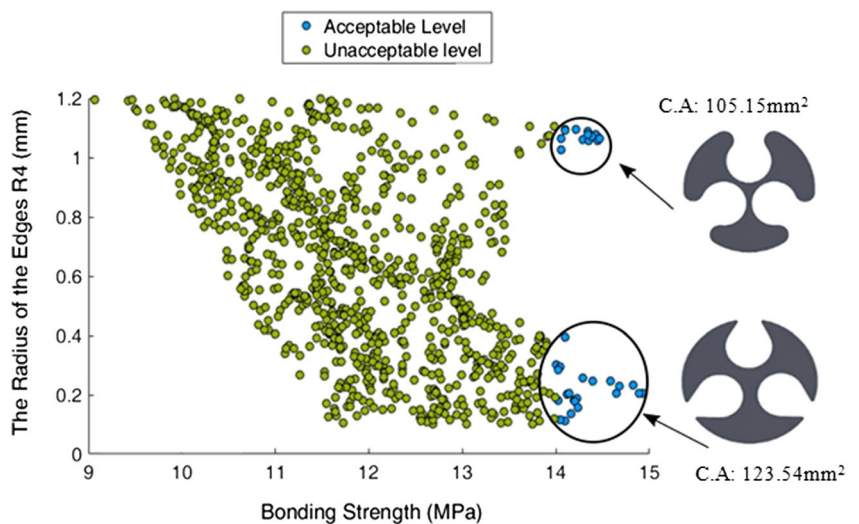
third of the examined samples have shown a bonding strength of about 12 MPa exceeding that found in the literature for the conventional rebar systems of 10 MPa (Shafaie et al. 2009). This means that the employed model in this report agrees well with that of the conventional systems and provides satisfactory results. On the other hand, the change in $R4$ and α have also provided very strong bond strength reaching a value of around 15 MPa which is very desirable. For the purpose of uncertainty and optimization, the acceptable level in the current investigation was taken above 15 MPa. This will reduce the number of samples that provide an acceptable level of bonding strength as well as provide the best bond performance which is higher than that obtained by standard rebar systems.

When plotting $R4$ against the bonding strength, Fig. 18, it can be seen that the highest bonding strength is observed at $R4$

values of 0.1–0.4 and 1.0–1.2 mm (circled). Moreover, when plotting the angle α against the bonding strength, Fig. 19, it can clearly be seen that the optimum strength is attained at angles between $50 - 70^\circ$.

In order to obtain a clear understanding of these results, a combined 3D plot was created as shown in Fig. 20. It has been observed that the best bonding strength was obtained at an angle of 60° . From a materials point of view in terms of cost saving, the value of $R4$ between 1.0–1.2 mm has resulted in a reduced cross sectional area of 105.15 mm^2 when compared to the original area of 113 mm^2 or to the area 123.54 mm^2 when $R4$ was 0.1–0.4 mm. This means that the values of $R4$ that will be considered will be those between 1.0–1.2 mm. This reduces the problem of optimisation and makes it simple to run the robust analysis as it will be discussed later.

Fig. 18 The radius $R4$ against the bonding strength (C.A. means the Cross-sectional Area)



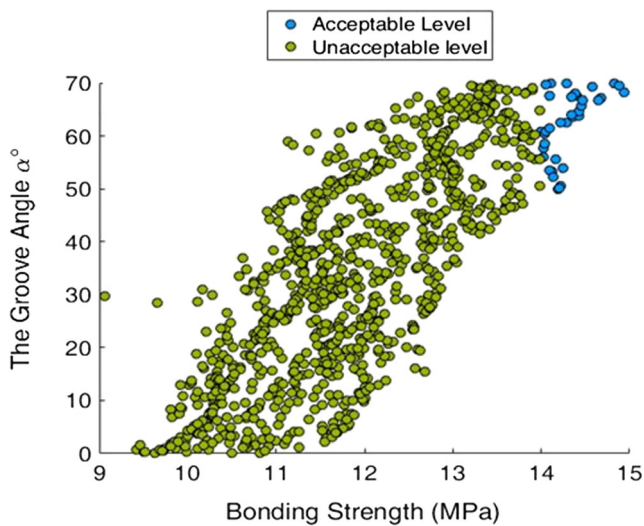


Fig. 19 The angle α against the bonding strength

5.5 The meta-model design optimisation

The Meta-model-based design optimisation is becoming increasingly popular in the industrial practice for optimisation of complex engineering problems, especially to reduce the burden of computationally expensive simulations. The idea behind the Meta-model-based design optimisation is to build a surrogate model (or a meta-model) from a reduced number of simulation runs and subsequently use the model for optimisation purposes (Gano et al. 2006). The surrogate model, i.e. $y = f(x_1, x_2, \dots, x_n)$, approximates the relationship between the design variables, i.e. x_1, x_2, \dots, x_n , and the output variable, y . This method can speed up the design optimisation process since the function evaluations of the surrogate model are less expensive to execute when compared to deterministic simulations. The simplest type of ‘Response Surface’ is a linear model in which the functional relationship $f(x_1, x_2, \dots, x_n)$ is assumed to be a linear function of the design variables. Linear models can be extended to polynomial response surface models wherein the response surface is a polynomial function of the design

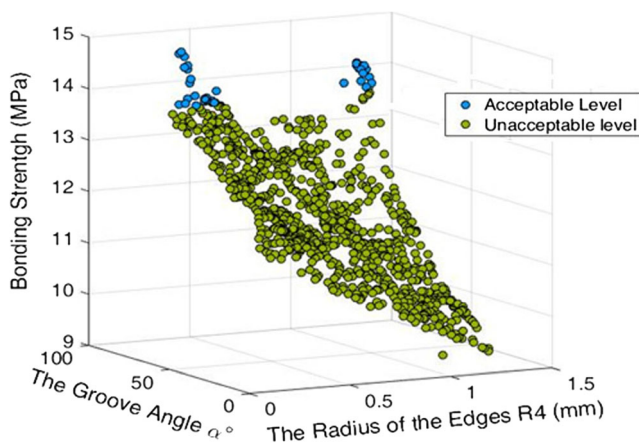


Fig. 20 A combined 3D of the radius R4, α and the bond strength

variables. In either way, the linear or higher order response surface (polynomials) can be obtained using the ‘Ordinary Least Squared’ approach by minimising the sum of the squared distances of a given data points from the surface. In this case, the surrogate modelling utilising the least squared approach assumes that all errors are normally distributed with given mean and variance. This assumption is often too stringent in real-world problems.

One of the most popular methods that falls under the Meta-model approaches is the Kriging (or Gaussian process interpolation). This is considered a surrogate model that is able to approximate the deterministic noise-free data and has proven to provide high level optimisation results alongside design space exploration, visualisation, prototyping and sensitivity analyses (Booker et al. 1999). The Kriging approach is an interpolation technique which differs from the conventional least squares approach as its model goes through each calculated point. With the Kriging method, it is possible to describe the uncertainty of the interpolation outside the given points (Ulaganathan et al. 2015). The widespread adoption of the Kriging method is due to the ability to approximate complex response functions (Martin and Simpson 2005) and less restrictive assumptions, compared to the least square method, on distribution of residual errors.

5.5.1 The ordinary kriging model

The Kriging method has been pre-fixed with different names depending on the form of the regression function, $f(x)$. For instance, the simple Kriging method assumes that $f(x)$ is a known constant, i.e. $f(x) = 0$. On the other hand, the ordinary Kriging approach assumes that $f(x)$ is constant but unknown, i.e. $f(x) = \alpha_0$. For more complex processes, trend functions might be linear or quadratic polynomials. In this regard, the universal Kriging treats the trend function as a multi-variate polynomial such that:

$$f(x) = \sum_{i=1}^p \alpha_i b_i(x)$$

Where $b_i(x) = b_1(x), b_2(x), \dots, b_p(x)$, are the basis functions (e.g. the power base for a polynomial) and $\alpha_i = (\alpha_1, \alpha_2, \dots, \alpha_p)$ denote the coefficients. The idea is that the regression function captures the largest variance in the data (the general trend) and then the Gaussian Process interpolates the residuals. In fact, the regression function $f(x)$ is actually the mean of the broader Gaussian Process Y .

5.5.2 The blind kriging model

One of the most widely used Kriging approaches is the Blind Kriging method. In this approach, the trend function $f(x)$ is unknown and is hard to choose for a given problem. Some

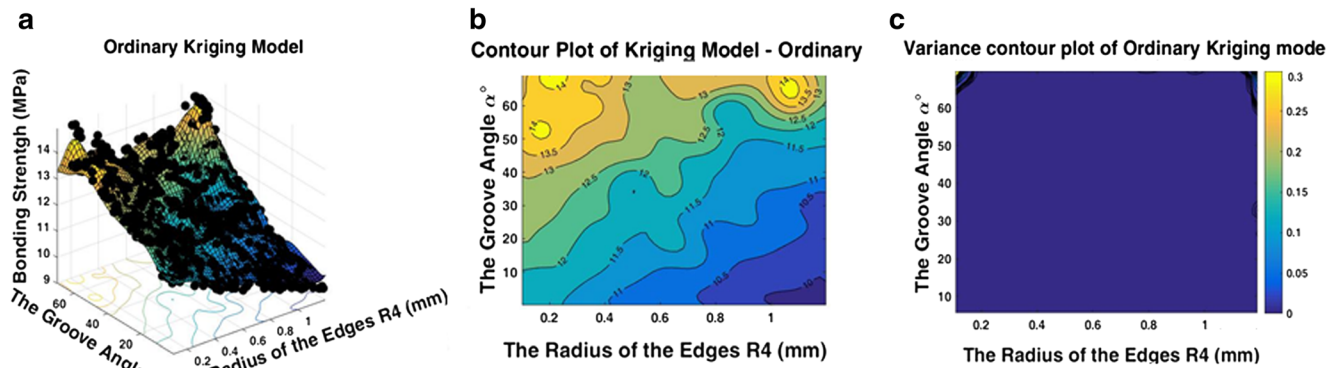


Fig. 21 (a) The Blind Kriging response surface, (b) The contour plot of the bonding strength, (c) The variance plot

feature selection methods sometimes offer the possibility to identify the most plausible interactions occurring in the data (Guyon & Elisseeff, 2003). The Blind Kriging is used to efficiently determine the basis functions, or features, that capture the most variance in the sample data. In this respect, a set of candidate functions is considered from which to choose for the problem. In the ideal case the sample data is almost fully represented by the chosen trend function and the stochastic process $Z(x)$ has little or no influence. The idea is to select new features to be incorporated in the regression function of this Kriging model, taking into account features that are already a part of the regression function of the model. The whole set of candidate functions that is used to fit the data in a linear model are given by:

$$g(x) = \sum_{i=1}^p \alpha_i b_i(x) + \sum_{i=1}^t \beta_i c_i(x)$$

where t is the number of candidate functions. The first part of this equation is the regression function of Kriging and, hence, the coefficients α have already been determined independently of $\beta = (\beta_1, \dots, \beta_t)$. The estimation of β provides a relevance score of the candidate features. A frequentist estimation of β (e.g., least-squares solution) would be a straightforward approach to rank the features (e.g. the least-squares solution) would be a straightforward approach to rank the features.

5.5.3 The co-kriging model

The Co-Kriging, a special case of multi-task or multi-output Gaussian Processes, exploits the correlation between fine and coarse model data to enhance the predictive accuracy (Kennedy & O'Hagan, 2000). Generally, creating a Co-Kriging model can be interpreted as constructing two Kriging models in sequence: a first Kriging model of 100 samples (the coarse data) followed by a second Kriging model constructed on the residuals of the 1000 samples (fine and coarse data). This is a useful technique since it uses a small set of samples to predict the long-term properties. This will be useful to save time and cost in relation to the required data since it is able to predict the overall behaviour within and outside the given range of properties.

These methods, i.e. the Ordinary, Blind and Co- Kriging will be employed in the current study to provide a comparative study of all techniques so as to capture the optimum regions of bond strength in the given case study. The purpose is to validate the obtained data as well as to provide the optimum and robust design of the parameters. These methods can be used to find the surrogate model that approximates the solution to the problem since it employs less stringent assumptions about the

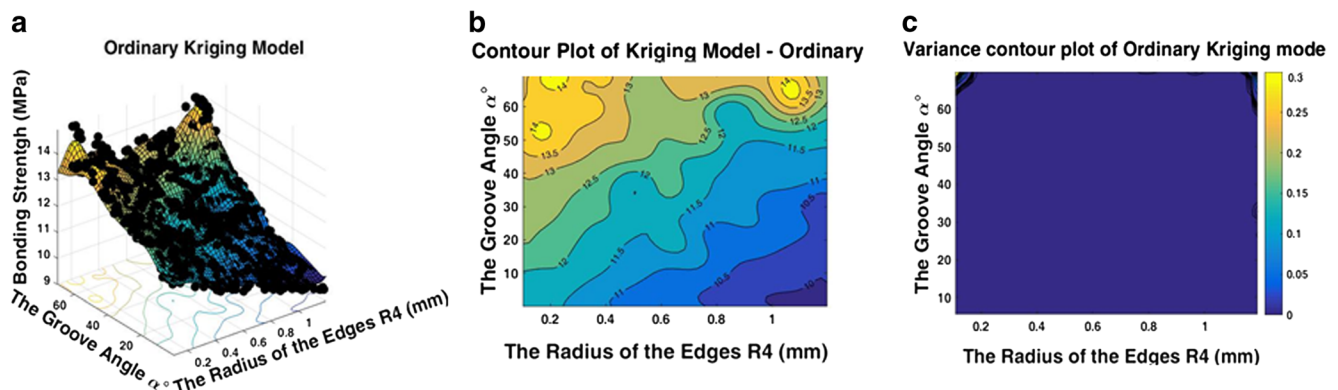


Fig. 22 (a) The Ordinary Kriging response surface, (b) The contour plot of the bonding strength, (c) The variance plot

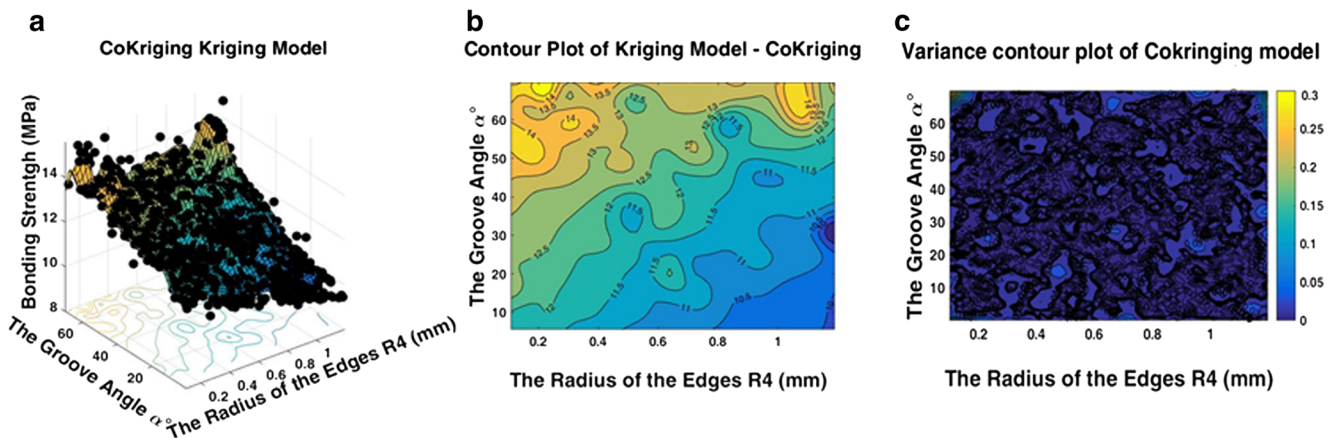


Fig. 23 (a) The Co-Kriging response surface, (b) The contour plot of the bonding strength, (c) The variance plot

residual errors and they are able to model complex systems. These models were built using the Design and Analysis of Computer Experiments (DACE) software toolbox (Couckuyt et al., 2013). The model DACE software package is a freely available toolbox which performs both calculations of the Kriging function and parameters optimisation. The Meta-model found using the various Kriging methods can then be used to identify the optimal regions of the bond strength. Subsequently, a global optimum zone can be found by applying the same methodology to the optimal regions.

5.6 The results of the various kriging applied to the re-bar system

The obtained results from the Blind, Ordinary and Co-Kriging are shown in Fig. 21, Fig. 22 and Fig. 23, respectively. The ‘Mean Squared Error’ of the Leave-out cross validation was chosen to evaluate the quality of the fit as well as the predictive capability of the technique. The Blind Kriging results, Fig. 21 (a), have provided a very good fit capability of the data with two optimum regions observed characterised by a dome-like response surface. These two optimum regions can be viewed more clearly in the contour plot of the response surface, Fig. 21 (b), wherein the highest bond strength is obtained, i.e. 14 MPa, at a groove angle between 50–70° and R4 range of 1–1.2 and 0–0.2 mm. In the variance plot, Fig. 21 (c), it can be seen that there is no variance between the actual data set and the predicted response surface which proves the high quality of the Blind Kriging method. On the

other hand, the results of the Ordinary Kriging, Fig. 22 show slightly different results. Despite the fact that the surface response plot, shown in.

Figure 22 (a), indicates a similar trend and provides similar optimum regions with groove angles between 50 and 70° and R4 values of 1–1.2 and 0–0.3 mm, Fig. 22 (b), it was unable to capture all the actual data set when compared to the Blind Kriging approach. The Blind Kriging provided a wider range for the optimum bond strength of 14 MPa when compared to the Ordinary Kriging. Moreover, the variance plot shows higher variance values especially at the corners, Fig. 22 (c), where the two optimum regions are located. This shows the inferior predictability as well as the low robustness obtained when this method was employed. When the Co-Kriging method was utilised, the poorest quality of the fitting was observed as shown in the response surface, Fig. 23 (a). It can be clearly seen that most of the points were not captured by the model along with a less robustness, i.e. range of the highest bond strength, obtained, Fig. 23 (b). Moreover, a huge amount of variance is observed when the variance contour plot was generated, Fig. 23 (c), almost in all regions.

Overall, it can be seen that the Blind Kriging has provided the best method to fit the data as well as interpolate the various gaps in the data set. Moreover, when the Mean Squared error analysis of the Leave-Out Cross Validation was employed, the error was the least for the Blind Kriging followed by the Ordinary Kriging and finally the Co-Kriging, Table 2.

Table 2 The associated errors for the Ordinary, Blind and the Co-Kriging methods using the Mean Squared error analysis of the Leave-Out Cross Validation

A Summary of the Associated Errors in all Methods		
Ordinary Kriging Method	Blind Kriging Method	Co-Kriging Method
200.0034×10^{-4}	0.0039×10^{-4}	6430.4812×10^{-4}

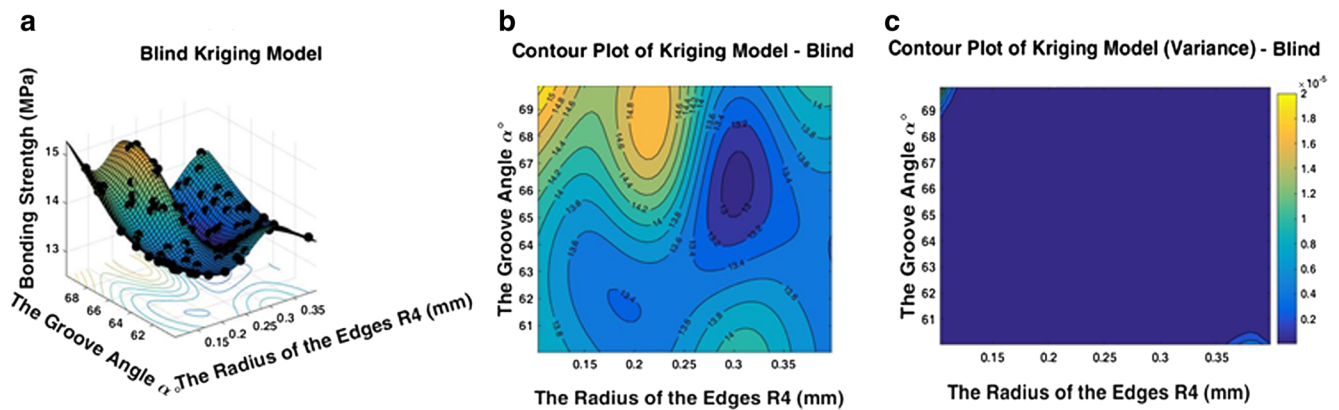


Fig. 24 The optimum left-hand side region of Fig. 74 obtained by the Blind Kriging: (a) The response surface, (b) The contour plot, (c) The variance plot

5.7 The optimum and robust Design of the Rebar System

From the above analysis, the Blind Kriging proved to be able to provide the optimum and robust design of parameters for the groove angle α and the edge radius R4 relative to the bond strength of the re-bar system. The two optimum regions of the response surface for the Blind Kriging, Fig. 21 (a), will be analysed at a closer level. Each region will be analysed individually so as to obtain the best set of parameters that provide the optimum and robust design. The first optimum region that is located nearer to the left-hand side of Fig. 21 is magnified and re-constructed here as shown in Fig. 24 (a). In order to show the excellent fit of this method, a further 100 samples were generated and projected onto the response surface. The contour plot, Fig. 24 (b), show the robust and optimum parameters located between R4 values of 0.2 and 0.25 and groove angle α between 67 and 70°. The variance is mostly negligible as can be seen in the variance contour plot, Fig. 24 (c).

On the other hand, when the right-hand optimum region of Fig. 21 was magnified and re-constructed, as shown in Fig. 25, a further 100 samples were regenerated and projected

onto the response surface. It is apparent that the response surface has captured all the projected data with very high accuracy (errors of magnitude 0.000039%), Fig. 25 (a). In the contour plot, Fig. 25 (b), it is evident that the optimum and robust design is located at R4 values between 1.0 and 1.1 along with groove angles between 61 and 70°. The variance contours, Fig. 25 (c), show a minimal amount of variance for the fit which is desirable for the robust design.

6 Conclusions

The Co-tropic rebar system has been investigated in terms of the optimum and robust design of the various parameters involved in its geometry. The sensitivity studies of the system have shown that the system is most sensitive to two parameters, namely: the groove angle α and the edge radius R4. These two parameters were thoroughly studied using uncertainty models and robust design analyses. The new advancement in the current study is the employment of a novel approach that links the ANSYS Workbench with MATLAB to generate thousands of data that have a normal

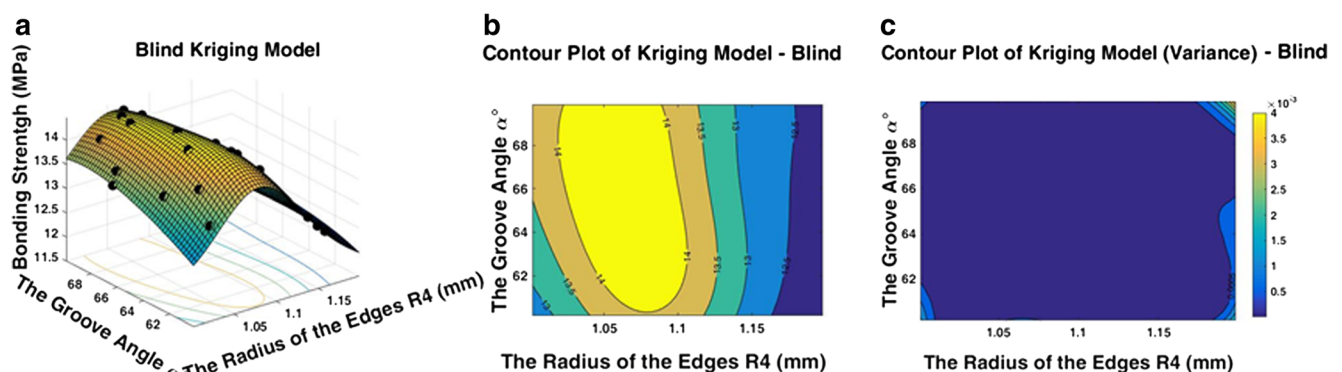


Fig. 25 The optimum right-hand side region of Fig. 23 (a) obtained by the Blind Kriging: (a) The response surface, (b) The contour plot, (c) The variance plot

distribution (using the Latin hypercube method). The best combination of α and R4 that has provided the maximum bond strength of 14 MPa with the concrete was identified. In order to better understand and validate the obtained results, the Kriging method was utilised to create the response surface. This approach has provided the robust design in 3D combination between the bond strength, α and R4. It has been observed that the best groove angle α lies in the region between 60° and 70° with edge radii of either 0.2–0.25 or 1.0–1.1 mm. This analysis was a very useful exercise that has employed the various uncertainty and robust design technique in order to optimise such a structure. This approach can be applied to any engineering application in order to save time and cost associated with such simulations. The predictive capability of the methods were assessed and compared against each other to increase the level of confidence in the obtained results.

Acknowledgements The funding provided by the ASTUTE 2020 project (Advanced Sustainable Manufacturing Technologies) based at Swansea University, the European Regional Development Fund through the Welsh Government and the Welsh European Funding Office (WEFO) is highly appreciated.

Compliance with ethical standards

Conflict of interest The authors declare that they have no conflict of interest.

Open Access This article is distributed under the terms of the Creative Commons Attribution 4.0 International License (<http://creativecommons.org/licenses/by/4.0/>), which permits unrestricted use, distribution, and reproduction in any medium, provided you give appropriate credit to the original author(s) and the source, provide a link to the Creative Commons license, and indicate if changes were made.

Publisher's Note Springer Nature remains neutral with regard to jurisdictional claims in published maps and institutional affiliations.

References

- ACI_Committee (2016) Bond and Development of Straight Reinforcing Bars in Tension, s.l.: ACI Committee 408.
- Aldoumani N et al. (2016) The robustness of carbon fibre members bonded to aluminium connectors in aerial delivery systems. *Cogent Eng* 3
- ANSYS (2009) Element Reference, s.l.: s.n
- ANSYS (2010) s.l.: Introduction to Contact, ANSYS Mechanical ANSYS Mechanical, Lecture 3
- ANSYS (2012) s.l.: ANSYS Mechanical APDL Theory Reference
- Barbosa M, Filho E, Oliveira T, Santos W (2008) Analysis of the relative rib area of reinforcing bars pull out tests. *Mater Res* 11(4)
- Booker, AJ, Dennis, JE, Frank, PD, Serafini, DB, Torczon, V., Trosset, MW (1999) A rigorous framework for optimization of expensive functions by surrogate. *Struct Multidiscip Optim.* 17(1):1–13
- Bryne D (1987) Taguchi approach to parameter design. *Qual Prog:* 19–26
- Doan M (2013) Advances in ANSYS R14.5 structural mechanics Solutions: 92
- Doyle J (2012) ANSYS. [Online] Available at: <http://www.ansys-blog.com/what-are-the-differences-between-the-contact-formulations/> [Accessed 3 May 2014]
- Gano SE, Renaud JE, Martin JD, Simpson TW (2006) Update strategies for kriging models used in variable fidelity optimization. *Struct Multidiscip Optim.* 32:287–298.
- Kabir M, Islam M (2014) Bond stress behavior between concrete and steel rebar: critical investigation of pull-out test via finite element modeling. *Int J Civ Struct Eng.* 5(1)
- Mahmoud A (2016) Finite element modeling of steel concrete beam considering double composite action [Journal], s.l.: Ain Shams Eng J., 1: Vol. 7.
- Martin J D, Simpson T. W (2005) Use of Kriging Models to Approximate Deterministic Computer Models, *AIAA Journal*, 43: 4
- Neto A, Rosa E (2008) Parametric uncertainty analysis considering metrological aspects in the structural simulation in viscoelastic materials. *Latin Am J Solids Struct* 5:75–95
- Padulo M (2008) Lecture notes in computational science and engineering: 271–280
- Ramakrishnan B (1991) A robust optimization approach using Taguchi's loss function for. *ASME*
- Ross P (1995) Taguchi techniques for quality engineering: loss function, Orthogonal Experiments Parameter and Tolerance Design
- Shafaie J, Hosseini A, Marefat M (2009) 3D Finite Element Modelling of Bond-Slip between Rebar and Concrete in Pull-Out Test. Tehran, The Third International Conference on Concrete and Development
- Taguchi G (1989) Engineering in production systems. Mc Graw Hill
- Thomas W (2011) Evaluation of novel fibre reinforcement by punch testing - A feasibility study [Report], s.l.: Concrete
- Ulaganathan, S, Couckuyt, I, Deschrijver, D, Laermans, E, Dhaene, T (2015). A Matlab Toolbox for Kriging Metamodeling.
- Wang L, Al E (2017a) A novel method of non-probabilistic reliability-based topology optimization corresponding to continuum structures with unknown but bounded uncertainties. *Comput Methods Appl Mech Eng* 326
- Wang L, Al E (2017b) Reliability estimation of fatigue crack growth prediction via limited measured data. *Int J Mech Sci* 121
- Wang L, Al E (2018a) Structural optimization oriented time-dependent reliability methodology under static and dynamic uncertainties. *Struct Multidiscip Optim:* 57
- Wang L, Al E (2018b) A novel methodology of reliability-based multidisciplinary design optimization under hybrid interval and fuzzy uncertainties. *Comput Methods Appl Mech Eng* 337
- You B (2013) Contact algorithm of finite element analysis for prediction of press-fit curve. *Info Comput Sci:* 2591–2600